Plant, Cell and Environment (2004) **27**, 685–695

On the mystery of the golden angle in phyllotaxis

S. KING[1], F. BECK[2] & U. LÜTTGE[3]

[1]*Department of Mathematics, Darmstadt University of Technology, Schlossgartenstrasse 7, D-64289 Darmstadt, Germany,* [2]*Institute of Nuclear Physics, Department of Physics, Darmstadt University of Technology, Schlossgartenstrase 9, D-64289 Darmstadt, Germany and* [3]*Insitute of Botany, Department of Biology, Darmstadt University of Technology, Schnittspahnstrasse 3, D-64287 Darmstadt, Germany*

ABSTRACT

Phyllotaxis, the arrangement of leaves around a stem, shows in the vast majority of cases a regularity in the divergence angle of subsequent leaves which divide the whole circle into regular fractions. These are in most cases rational fractions of two Fibonacci numbers in an alternating series, converging towards the irrational limit of the golden section, corresponding to the golden divergence angle of 137.5 . . . degrees. This peculiarity was a long-standing mystery. Here, it is related to the evolutionary pressure of optimal light capture for maximal photosynthetic activity. A model is established which relates minimal shadowing for the lower leaves to the divergence angle. Numerical results of this model agree well with semi-empirical data on the dependence of light capture from the divergence angle. The basic shadow function of the model is also related with the demand of minimal shadowing for the angular separation of leaves and obtain, using elementary number theory, as solution the golden section. Further numerical studies show that the rational approach to the golden section (Schimper–Braun series) is related to the leaf width and the number of leaves of the plant.

Key-words: golden angle; leaf canopy; light capture; number theory; optimization; phyllotaxis; Schimper–Braun series.

INTRODUCTION

The angular position of leaves follows spiral arrangements around the stem (Sitte 1998). This phyllotaxis obeys rules which in the vast majority of higher plants (approximately 250 000 species) divide the divergence angle of subsequent leaves into regular fractions of the whole circular angle of 360° (Cummings & Strickland 1998). It is a long-standing observation that these fractions belong to a series where numerator and denominator are Fibonacci numbers, for example, 1/2, 1/3, 2/5, 3/8, 5/13, . . . [Schimper–Braun principal series, Adler, Barabe & Jean (1997)]. The series converges to the irrational limit of the 'golden section' 0.382 . . . , which corresponds to the 'golden angle', $\alpha = 137.5\ldots°$ (see Fig. 1). There is a vast literature on this phenomenon, starting with observational phyllotaxis (Bonnet 1754), followed by mathematical phyllotaxis in the first half of the nineteenth century with the pioneering work of Braun (1831), Schimper (1836) and Bravais & Bravais (1837). Almost as numerous are the attempts to understand the building principle of this series (for a rather complete survey, see Jean 1994). A convincing explanation why phyllotaxis follows the rational Fibonacci series is, however, still missing. Recent attempts, based on the Gierer–Meinhardt activator–inhibitor model can produce a regular series (Meinhardt 1984) by adjusting parameters properly. This describes how plants grow, but does not explain why nature chooses the Shimper–Braun series, or the golden angle. It has even entered leading textbooks (Sitte 1998) that the concept of the Schimper–Braun principal series has hampered understanding of phyllotaxis more than supporting it. The mysterious connection that might exist between nature's construction principles and the aesthetic concept of the 'golden rule' always remained intriguing.

It has been argued (Adler *et al*. 1997; Sitte 1998; Cummings & Strickland 1998; d'Ovido & Mosekilde 2000) that leaf arrangements are the simple result of an optimal, that is densest, packing of the leaf buds on the growth cone of the shoot axis as determined by morphogenous signalling compounds in the apex. However, the problem of finding the densest packing of finitely many objects is very difficult from a mathematical point of view. Mathematicians studied the problem of finding densest packings with respect to various notions of density (e.g. the parametric density). However, even for the basic problem of packing a finite number of unit circles into a disc-shaped container of minimal radius there is no hope for a general solution (Fejes Tóth 1953; p. 157 onwards). Exact results are only known for a small number of circles (Kravitz 1967; Melissen 1994). Although the optimal packing of infinitely many unit circles in the plane is a regular hexagonal lattice, it is known that finite densest packings have no lattice symmetry, for many typical notions of density (Schürmann 2002). Of course, the problems become even more difficult and the densest packings even more irregular when one tries to pack circles of different size. In some cases, it is optimal to pack small circles into the gap between adjacent large circles (Fejes Tóth 1953; pp. 71–79). This packing strategy is not compat-

Correspondence: F. Beck. E-mail: freder.beck@physik.tu-darmstadt.de

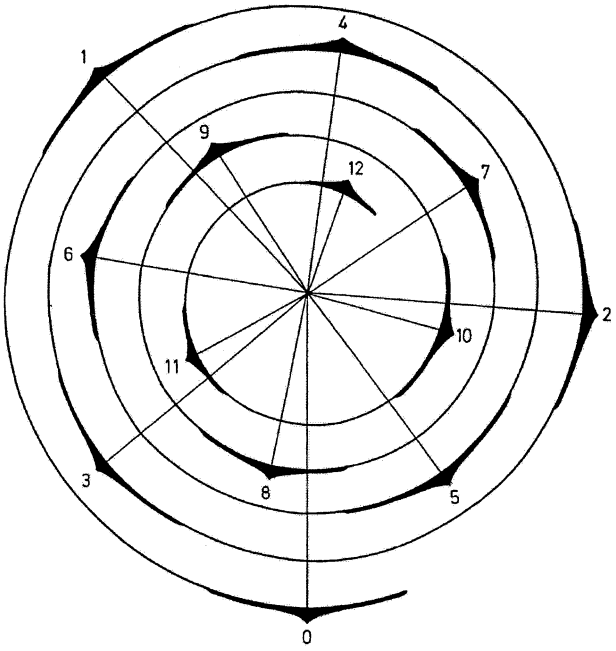

Figure 1. Disperse leaf arrangement. The example chosen is *Adenocaulon bicolor* using the leaf angle given in Pearcy & Yang (1998). Successive leaves in the spiral are numbered.

ible with the arrangement of leaf primordia on the growth cone. Certainly, in order to produce a good packing, it is good heuristics to arrange the successive leaf buds according to the phyllotactical spiral. We are, however, not convinced that phyllotaxis is the result of an optimal solution of any classical mathematical packing problem, unless the growth parameters of the leaf buds are very specially and carefully chosen. Thus it seems difficult to explain in that way the regularity of the phyllotactic spiral by optimal packing arguments. We also remark here that one of the main characteristics of phyllotaxis is fivefold symmetry, banned from regular crystal growth by the crystallographic restriction (Jean 1994).

Here we first establish a model that optimizes light capture of the plant under limiting light conditions, as prevails, for example, for forest understorey plants. This guarantees maximal photosynthetic activity, and hereby maximal carbon gain. Pearcy & Yang (1998) showed by computer simulations based on empirical data that the light capture for the Redwood forest (Northern California) understorey plant *Adenocaulon bicolor* is optimal for a divergence angle very close to the golden angle. The maximum of their simulated light gain curve lies at 136.7°. Thus, strong evolutionary profit explains the occurrence of divergence angles close to the golden angle in nature. Our model reproduces these empirical results almost perfectly.

Our paper is organized as follows. We start with the formulation and motivation of our model for light capture and shadow cast. Then, we evaluate the model numerically and compare it quantitatively with the empirical results of Pearcy & Yang (1998). We study the influence of the model parameters on the qualitative behaviour of the results. In the final part we consider a simplified version of the model that allows for an analytic solution. We show by using abstract number theory that the golden angle assures maximal light capture of the leaves. Besides the mathematical beauty of this analytical solution, it shows why nature, in its evolutionary course, chose the golden angle, the most irrational number, as the ultimate goal of ecological optimization.

METHODS

The model

Our model is based on the observation that most plants grow towards the light. Hence, normally light comes in roughly parallel to the shoot axis, at least on average. For plants that do not match this condition, optimal light capture may be obtained by a distorted phyllotactic spiral. An example is provided by the horizontally turned needle leaves of the fir (Adler *et al*. 1997). We keep the model as simple as possible in order to bring out the salient features of optimizing light capture in a clear way, and to guarantee generality, independent of special plant morphologies. One could employ, of course, different and especially more complex model assumptions. We justify, however, our model with the almost perfect reproduction of the semi-empirical results of Pearcy & Yang (1998).

We denote the divergence angle of spirally growing leaves by $\alpha = x \cdot 360°$, with $0 \le x \le 1/2$, and number the leaves successively, starting with the oldest leaf, i.e. with zero at the bottom: 0, 1, 2, . . . n, . . . (Fig. 1). The angular distance $w(n,x)$ between the n-th leaf and the 0-th leaf is given by

$$w(n,x) = |x \cdot n - [x \cdot n]| \cdot 360° \qquad (1)$$

where $[x \cdot n]$ stands for the integer next to $x \cdot n$. The shadow cast by the n-th leaf on the 0-th leaf is denoted by $s(n,x)$. Then the total shadow on the 0-th leaf is, of course, the sum of $s(n,x)$ over n.

We now introduce two model assumptions for the shadow function $s(n,x)$

i Since the light comes predominantly in parallel to the stem, $s(n,x)$ is minimal if $w(n,x) = 180°$, and maximal if $w(n,x) = 0°$. The maximal value is assumed to be constant for $w(n,x) \le B$ ('zero point shadow'). The constant $B > 0$ combines several physiological and environmental parameters: leaf width (because the shadow function $s(n,x)$, Eqn 2, starts to decrease only for $x > B$); leaf transparency (since the leaf on top of another is not completely opaque); light diffuseness (because scattered light and light incident not exactly parallel to the stem reaches the lower leaf independently of higher up leaves). We treat B as one of the three fit parameters of the model and do not attempt to calculate it from the physiological conditions, which anyhow depend on the special species and its environment. The constant $B > 0$ therefore has the meaning of an effective leaf width. The

least bias ansatz is $s(n,x) \sim 1/\mathrm{Max}\{w(n,x), B\}$. This guarantees a smooth fall-off of the shadow from its maximal value $1/B$ to the minimum at $x = 1/2$.

ii In natural light the shadow cast by an object becomes weakened by non-directional diffuse light with increasing distance. In addition, with increasing n the leaf area tends to decrease, since the leaves are younger. So we assume $s(n,x) \sim 1/n$.

Conditions (i) and (ii) lead to the form

$$s(n,x) = \frac{c}{n \cdot \mathrm{Max}\{w(n,x), B\}} \tag{2}$$

The meaning of the scaling constant c will be discussed after the introduction of the light capture function $L(x,B)$ below. In order to obtain the total shadow which is thrown on the 0-th leaf, we have to sum over all leaves n above the 0-th leaf.

$$S(x,B) = \sum_{n=1}^{n_{\max}} s(n,x) \tag{3}$$

where $n_{\max}$ depends on the plant height. The light capture function is then given by

$$L(x,B) = S^{-1}(x,B) \tag{4}$$

The model is characterized by three constants, the effective leaf width, B, the scaling constant, c, and the number of leaves above the zero leaf, n_{max}. These constants have to be adjusted to the given conditions for a specified plant and its environment. There enter: the light conditions (average angle of incidence, amounts of direct and diffuse light), and the physiological conditions of light absorption efficiency of the plant. For details, see Pearcy & Yang 1996, 1998). The minimum light absorption for two completely overlapping leaves on top of each other ($n = 1$, $x = 0$) is B/c.

RESULTS

Numerical analysis

We first compare our model with results, which Pearcy & Yang (1998) obtained from empirical studies. These authors investigated the understorey plant *Adenocaulon bicolor* under a Redwood forest canopy. Utilizing the three-dimensional canopy architecture model YPLANT (Pearcy & Yang 1996) they were able to transform their empirical data, obtained from 10 selected plants, into numerical data on plant geometry, photon flux density (PFD), and light capture efficiency. In addition they were able, by changing the geometric parameters of the model, to study variations in the light capture efficiency for hypothetical plants with differing geometric parameters, notably differing divergence angles of the leaves.

Figure 2 shows the comparison of our model calculations with the semi-empirical data on the efficiency of light absorption as a percentage of the photon flux density (% PFD), obtained with YPLANT (Pearcy & Yang 1998). The data present the mean and standard deviation for 10 plants in its dependence on the leaf divergence angle α. The continuous curve shows the light capture function of our model, Eqn 4, evaluated for the same angular region as presented in Pearcy & Yang (1998). Fixing the scaling constant c of Eqn 4 by least squares fit to the data, our *a priori* model reproduces the empirical light absorption in its dependence on the divergence angle α for the understory plant *A. bicolor* very closely. Even the second (local) optimum of our model at $\alpha \approx 103°$ is found in the empirical study of Pearcy & Yang (1998) as well. The peak structure of the light capture function will be discussed in connection with the simplified version of the model, introduced in the next but one section.

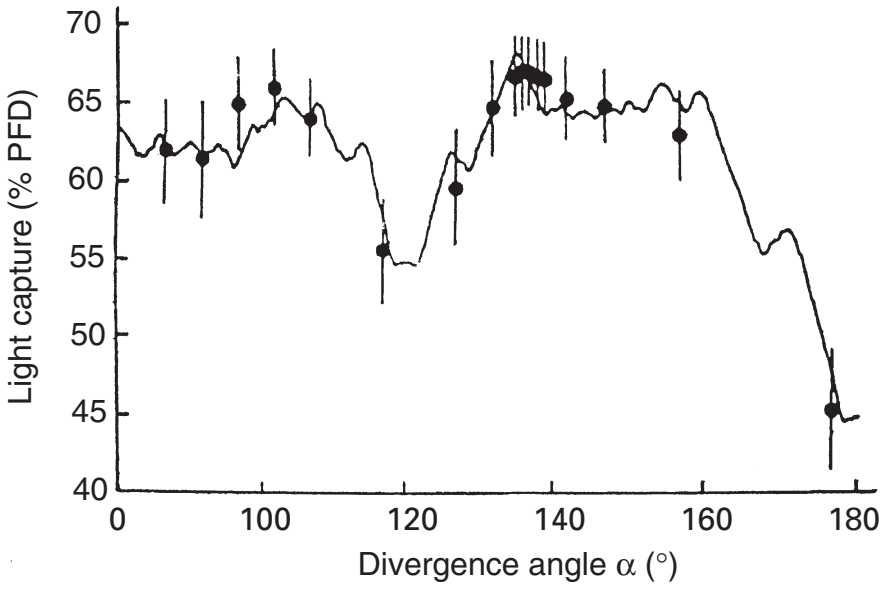

Figure 2. Comparison of empirical and simulated light capture in its dependence on the divergence angle α. Data show the percentage light capture (% PFD, photosynthetic efficiency of the photon flux density; Pearcy & Yang 1998). The points give the mean, and the error bars the standard deviation of 10 independent runs on samples of *A. bicolor*. The continuous curve represents the simulation in our model. In addition to the absolute maximum around the golden angle ($\alpha \approx 137.5°$) there occurs a second, relative maximum around 103°. Parameters in the calculation are: $B = 25°$; $c = 9.8 \times 10^{-2}$ from scaling to empirical percentage light capture; number of leaves above leaf number 0 (Eqn 3), $n_{\max} = 15$ which was the maximal node number observed by Pearcy & Yang (1998) (not a critical value if light capture is properly scaled, cf. Fig. 3).

Robustness of the model

Here, we present a sensitivity analysis with respect to variation of the parameters in the model to see how robust the model is with respect to parameter changes and how sensitive it is with respect to a simplification which is essential for the application of number theory in the next section. We also study the relationship between the effective leaf width and the members of the Schimper–Braun series.

The number of leaves in the summation over leaves on top of the lowest one, n_{max} in Eqn 3, is an open parameter, depending on the plant under investigation. We therefore study the light capture curve in its dependence on n_{max}. The result is shown in Fig. 3. Figure 3a shows a sequence of seven runs with, from top to bottom, increasing values of n_{max} in steps of 5. Of course, the light capture at the lowest leaf decreases with the number of leaves higher up, but the curves converge rapidly to an asymptotic form. This is reflected in the narrow spread of light capture curves in Fig. 3b, where the curves are scaled to the data by adjusting the free parameter c in Eqn 2. Thus, leaf number is not a critical parameter for the shape of the light capture curve as a function of the divergence angle.

Next, we study the influence of fluctuations in the individual divergence angles of the leaves. Pearcy & Yang (1998) sampled 10 plants from representative microsites in the Redwood forest. Naturally, they observed variations in the plant geometry, notably in successive leaf angles. We have simulated fluctuations in the leaf angle by allowing angular fluctuations by replacing Eqn 3 with

$$S(x,B) = \sum_{n=1}^{n_{max}} s(x + \mathrm{Random}[\pm\,\delta\alpha/360], n, B) \qquad (5)$$

where the function 'Random' generates random numbers in the interval $\{-\delta\alpha,\ \delta\alpha\}$. Figure 4 shows the results for fluctuations in the divergence angle α of ±5°. This value of

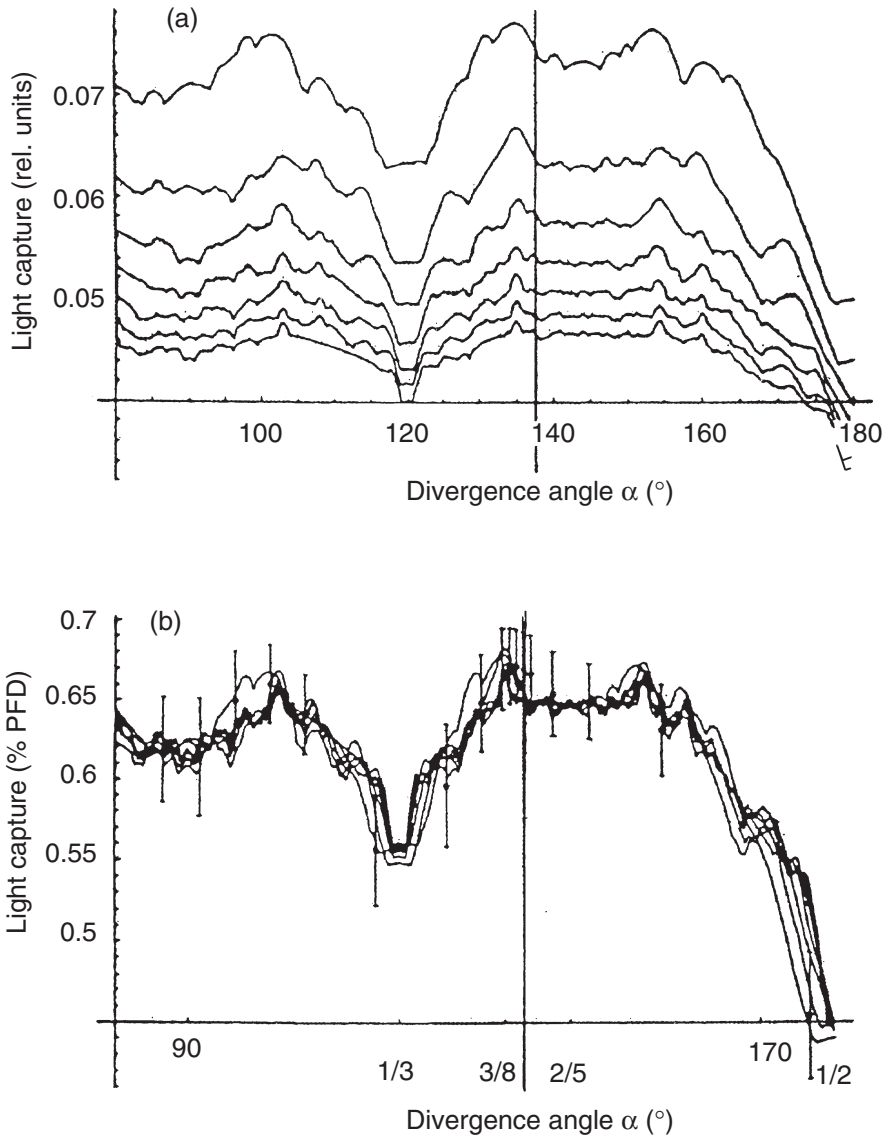

Figure 3. Dependence of the light capture function on the number of leaves above the bottom leaf. (a) Simulations for increasing leaf numbers from top to bottom, $n_{max} = 10 \ldots 40$, in steps of 5, and in relative units, obtained by setting the scaling constant in Eqn 2 to $c = 1$. (b) The same results scaled by adjusting the constant c of Eqn 2 to the data, together with the data (diamonds and error bars; Pearcy & Yang 1998). Effective leaf width in all simulations, $B = 25°$. The golden angle is marked by the vertical line. In (b) the first four Schimper–Braun ratios are marked on the abscissa.

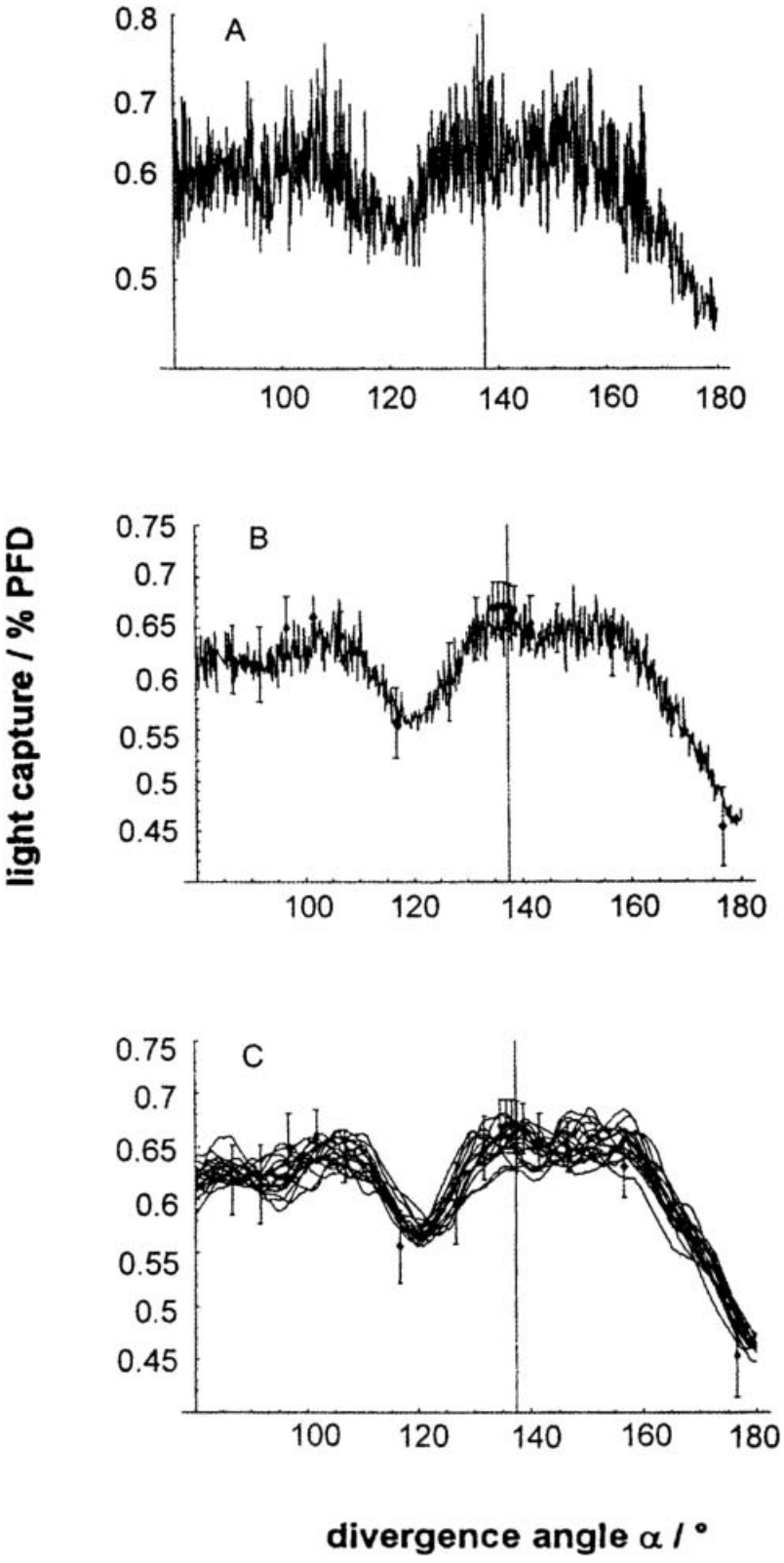

Figure 4. Fluctuation studies with our model. (A) Adding divergence angle fluctuations of ±5° to the average divergence angle according to Eqn 5 for a single run. (B) The same averaged over 10 independent runs. (C) Since the average of 10 independent runs with fluctuations fluctuates itself with each set of the 10 runs we present here the spread of 20 different evaluations of the mean of 10 runs each with fluctuations. This represents most closely the situation of the samples in the field study of Pearcy & Yang (1998). (B) and (C): Diamonds and error bars represent the data of Pearcy & Yang (1998). The golden angle is marked by the vertical line, and the constant *c* is adjusted to the data.

$\delta\alpha$ is about the maximal angular deviation which does not destroy the structure of divergence angle variation of the light capture curve, as shown in Fig. 4a for a single run. Averaging over 10 runs, Fig. 4b, we simulate the situation of Pearcy & Yang (1998). Calculating the standard deviations of the 10 runs presented in Fig. 4b, they cover a range of 0.02–0.06, in rough accordance with the empirical findings. Since the fluctuations introduce a stochastic element into each of the simulation runs, even the average over 10 runs (corresponding to the situation as employed by Pearcy & Yang 1998) fluctuates for each individual set of the 10 runs. In Fig. 4c we present the result of 20 different evaluations of the mean of 10 runs with fluctuations. The overlaid curves show that the uncertainty introduced by the angular fluctuations remains roughly within the width of the experimental error bars.

Numerical study of a simplified model

The sum over n leaves in the shadow function (Eqn 3) introduces a difficulty for analytic studies, such as presented in the number theoretical analysis. It also obscures somewhat the significance of analysing the occurrence of discrete maxima in the light capture in its dependence on the divergence angle. Because of this, we introduce the following simplification of our original model: instead of the sum over all leaves, we take as representative for the total shadow the shadow thrown by the most shadowing of all the n_{max} leaves onto the 0-th leaf

$$S_{rep}(x,B) = \mathrm{Sup}_n\, s(n,x) \qquad (6)$$

where 'Sup_n' denotes the supremum of $s(n,x)$ with respect to n, namely the maximal member of the set of all n_{max} values of $s(n,x)$ at fixed x.

By the same token, the light capture function, $L(x,B)$ (Eqn 4), is replaced by

$$L_{rep}(x,B) = S_{rep}^{-1}(x,B) = c\ \mathrm{Inf}_n[n \cdot \mathrm{Max}[w(n,x),B]] \qquad (7)$$

where 'Inf_n' denotes the inferior of $s(n,x)$, namely the minimal member of the set. This is, because of the inverse relation of S_{rep} and L_{rep}, the selection operation for the most shadowing leaf leading to minimal light capture.

This simplification gives a skeleton version of our model, which is useful for analytic studies since the main characteristics of the light capture curve are preserved as demonstrated in Fig. 5. Here we compare the full model (Fig. 2) with the smoothed result of the light capture function, Eqn 7. This shows that the essential structure of the light capture in its dependence on the divergence angle α is indeed also present in the skeleton version; that is, the main peak in the vicinity of the golden angle, the second peak slightly above 100°, and the shoulder to the right of the main peak. The fall-off towards small and large divergence angles is, however, much stronger than in both, the full model and the empirical data, indicating that the summation over all leaves smears out the light capture over a larger angular range.

A qualitative discussion of the dependence of light absorption on the divergence angle $360\,x°$ can give insight into the mechanism of leaf arrangement. The minimal value of Eqn 7 with respect to n for very small but finite B is obtained when leaf n overlaps almost totally with leaf 0. According to Eqn 1, $n \cdot x$ then must be close to an integer, so $w(n,x)$ is close to zero, and the shadow function $s(n,x)$ (Eqn 2) takes its maximal value $1/B$. For the lowest Schimper–Braun ratio, $x = 1/2$ ($\alpha = 180°$), this is already the case for leaf number 2. Consequently this ratio is for small B a highly unfavourable leaf arrangement. For the higher members of the Schimper–Braun series ($x = 1/3,\ 2/5, \ldots < 1/2$) the steadily increasing denominators (which represent the number of turns in the spiral until total overlap is again reached) shift this to increasingly higher n, and the factor n in Eqn 7 leads to increased light capture. This is the effect of the factor $1/n$ in the shadow function which

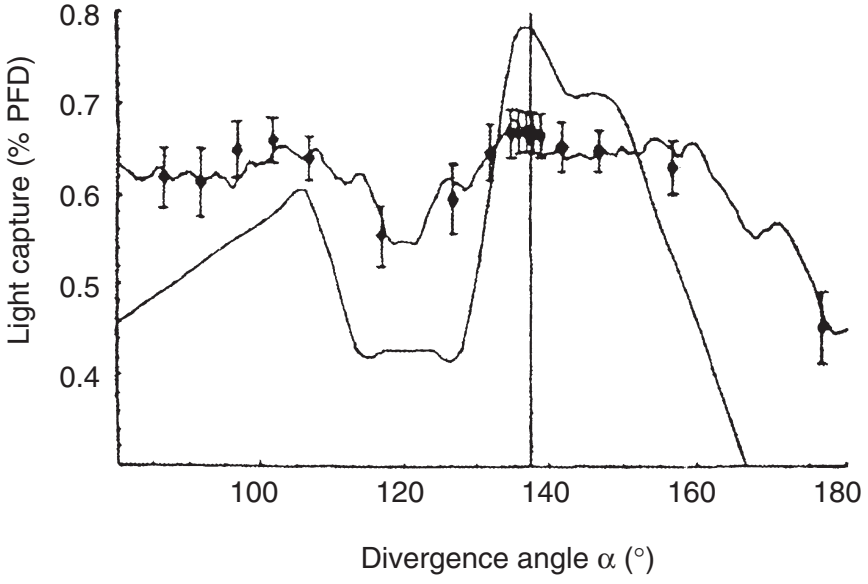

Figure 5. Comparison of the full (line close to data points), Eqn 4, and the simplified (line with more pronounced maxima and minima), Eqn 7, models, together with data. Percentage light capture is scaled by adjusting scaling constants c to the empirical data, and smoothing of the piecewise linear angular dependence of the simplified model is obtained with third order polynomials to ease comparison with the full model and data. Full model, $n_{max} = 15$, effective leaf width in both models, $B = 25°$. The golden angle is marked by the vertical line.

weakens the shadow thrown on the 0-th leaf the more higher up the shadowing leaf is located, and, in this way, the light capture increases. For larger B this sharp consequence for $B \to 0$ is weakened because the increased angular range B of constant shadow with simultaneously reduced shadow strength, $1/nB$ (Eqn 2) allows a lower n for optimal light capture. Through this effect, the preference of a special member of the Schimper–Braun series depends on the effective leaf width B.

This situation is shown quantitatively in Fig. 6. Figure 6a presents four light capture functions (without smoothing) for successively decreasing effective leaf widths. It is clearly seen how the angular structure breaks up from the rather unspecific dependence at $B = 40°$ to fine-structured peaks in the angular distribution for decreasing effective leaf width with a shift of the absolute maximum towards the golden angle. The lower Fibonacci-fractions of the Schimper–Braun series are successively more suppressed in the amount of light capture with decreasing effective leaf width. For $B = 5°$ only the golden angle is optimal, in agreement with the number theoretical result for $B \to 0$. There are also two peaks, around 110° and 150° (the lower one also prominent in the data of Pearcy & Yang 1998), which are not related to Schimper–Braun fractions. Figure 6b shows the selection of Schimper–Braun ratios quantitatively. Here we calculated the (unscaled) light capture $L(x_s,B)$ at discrete angular points x_s for the first 10 members (x_1 to x_{10}) of the Schimper–Braun series. For effective leaf width $B = 20°$ the light capture reaches its maximal value already for a low phyllotactic fraction whereas for $B = 1°$ the maximum is reached only very closely to the golden angle ($55/144 \times 360° = 137.5°$).

It is instructive to study the occurrence of the peak structure in the light capture function as the number of leaves above the bottom leaf increases. This is shown in Fig. 7a. The total number of leaves above the bottom leaf is successively increased from 2 to 8. For $n = 2$ (three leaves in total) light absorption is not, as could be expected, optimal for

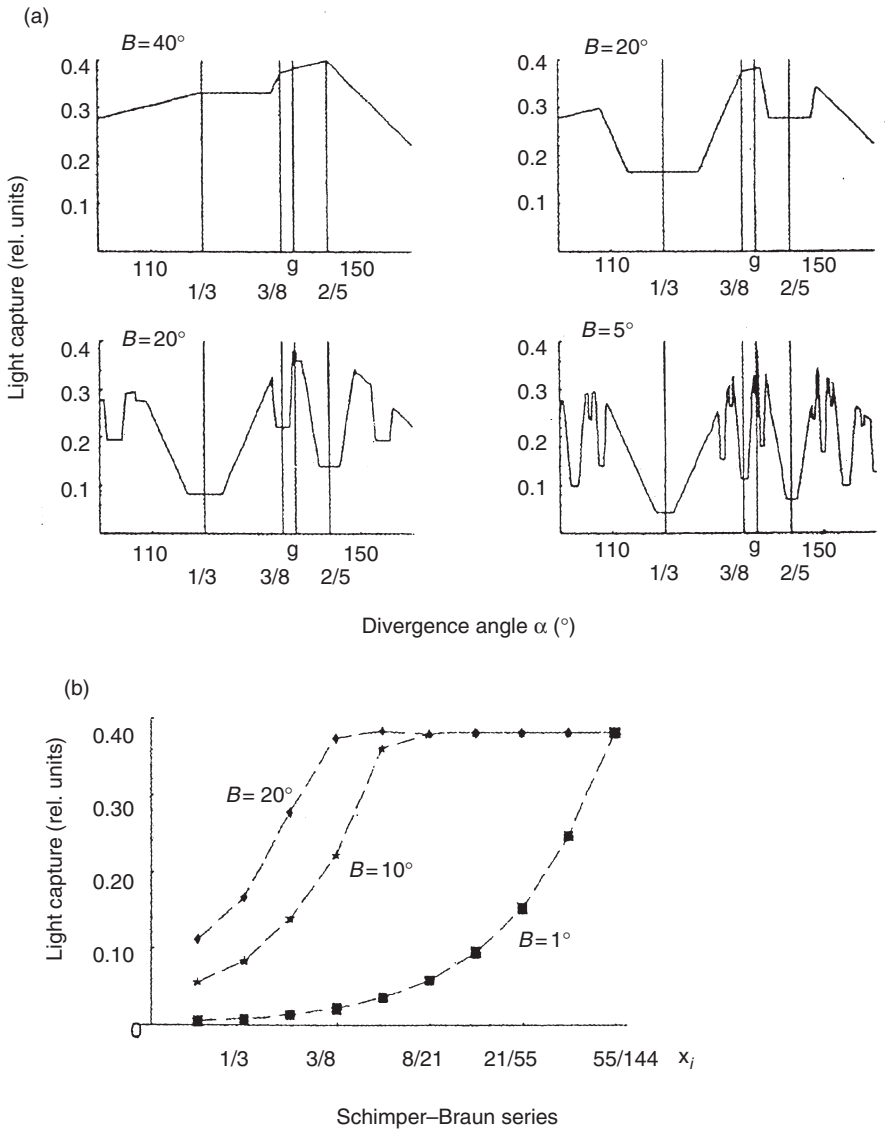

Figure 6. Increasing sensitivity of the light capture with decreasing effective leaf width in the simplified model. (a) Light capture in relative units ($c = 1$ in Eqn 2) as function of the divergence angle for four different effective leaf widths B. The angles of the Schimper–Braun series are marked by their fractions (angle = fraction times 360°), and the golden angle by g. The suppression of the light capture at the lower Schimper–Braun fractions with decreasing effective leaf width is clearly seen. (b) Light capture (full model) at discrete values of the Schimper–Braun series, x_i, for three different values of B. The highest Schimper–Braun ratio, $x = 55/144$, is already up to second and higher decimals equal to the golden section g = 0.382. . . .

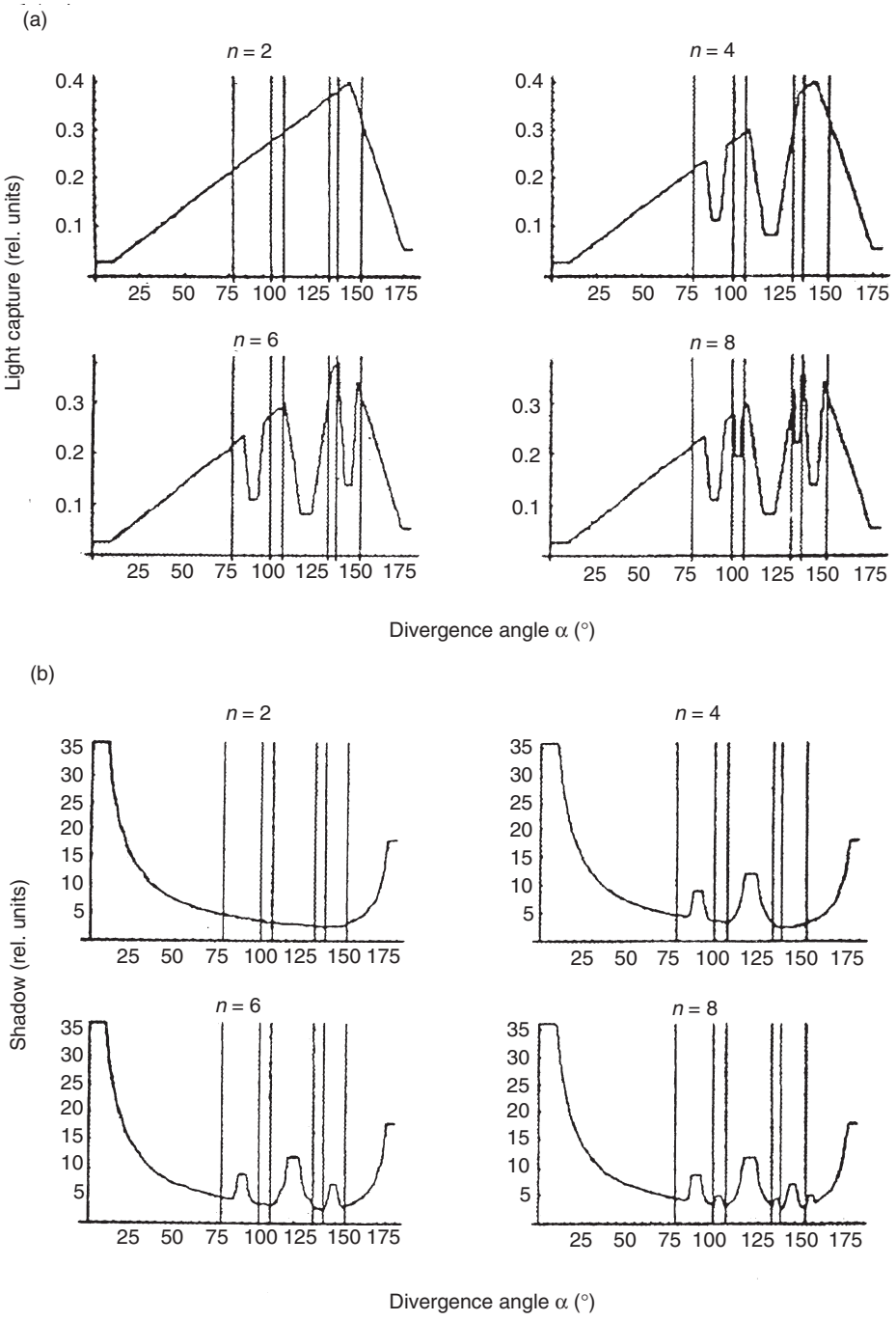

Figure 7. (a) Light absorption functions (Eqn 7), and (b) shadow functions (Eqn 6; relative units) in their dependence on the divergence angle and the number, n, of leaves above leaf zero for $n = 2 \ldots 8$ (total number of leaves is $n + 1$). Effective leaf width $B = 10°$, scaling constant $c = 1$. The vertical lines in each diagram denote the endpoints of the Fibonacci type series presented in Table 1.

$\alpha = 120°$ (tristar positioning of the three leaves), but shifted towards a larger divergence angle. The reason for this is the weakening of the shadow thrown from the higher-up leaves in the spirally growing plant which optimizes light absorption for a larger separation of the close-by leaves. As can be seen from the later diagrams in Fig. 7a, this effect is crucial for the occurrence of the peak structure for increasing total leaf numbers, and thus also for the absolute optimum at the golden angle.

From total leaf number six onwards the structure of the light absorption curve is practically stable, resulting in four peaking groups around 70°, 100°, the golden angle and 150°. The absolute optimum is the golden angle at $\alpha = 137.5 \ldots °$. The relative optima are members of less pronounced series, cf. Table 1. Next to the Schimper–Braun series ranges the Lucas series, found in about 2% of sampled species (Jean 1994), and reflecting itself in the data as well as in the model with the peak $\alpha \approx 100°$. The number theoretical analysis (cf. Eqn 8 below, and Appendix) shows that the optimum for the divergence angle will be obtained for a continued fraction expansion of the divergence angle which contains coefficients as small as

Table 1. Table of Fibonacci-like series

Continued fraction	First three rationals	Asymptotic divergence angle (°)	Series classification
[0,2,1,1,...]	1/2, 1/3, 2/5,...	137.508 ... golden angle	Schimper–Braun series
[0,3,1,1,...]	1/3, 1/4; 2/7,...	99.502 ...	Lucas series
[0,2,2,1,1,...]	2/5, 3/7, 5/12,...	151.136	anomalous
[0,3,2,1,1,...]	2/7, 3/10, 5/17,...	106.447 ...	not classified
[0,4,1,1,1,...]	1/4, 1/5, 2/9,...	77.955 ...	normal
[0,2,1,2,1,1,...]	3/8, 4/11, 7/19,...	132.178 ...	not classified

The first digits after the zero (which defines the rationals as <1) are successively increased beyond the optimal Schimper–Braun series which leads asymptotically to the golden angle. The first column presents the continued fraction expansions (see Appendix) of the irrational limits. For the series classification (last column), see, for example, Jean (1994).

possible. So, the golden angle separation is characterized by the expansion $x_{opt} = [0,2,1,1,1,\ldots] = (3 - \sqrt{5})/2$. Following this number theoretical result, we can obtain the next optimal divergence angles by successively increasing the first digits beyond $a_0 = 0$ and $a_1 = 1$ (which restricts the partial quotients, see Appendix, to the interval [0, 1/2] in the continued fraction expansion. In this way, we obtain the six values, corresponding to relative optima, as marked by vertical lines in Fig. 7. It should again be emphasized, however, that the vast majority of plant species (> 90%) follow the Schimper–Braun series, asymptotically leading to the golden angle. In reality, of course, the discrete and piecewise linear peaking structure of our simplified model is smoothened by the unavoidable fluctuations and irregularities in the plant growing process (cf. Fig. 5).

Also of interest is the shadow function for the same sequence of total leaf numbers, as shown in Fig. 7b. Again, for n larger than 6 the situation stabilizes, and the shadow looks like acting as a barrier between optimal areas for light absorption, that is, minimal shadow.

The diagrams of Fig. 7 provide direct evidence that our model expresses the essential features of the evolutionary pressure towards maximal photosynthetic activity. It is, however, an open question how this evolutionary preference is implemented in actual growth dynamics through genetic and biomolecular mechanisms.

Number theoretical analysis

We determine the optimal divergence angle $\alpha_{opt} = x_{opt} \cdot 360°$ from the requirement of maximal light capture for the 0-th leaf, which, due to symmetry, is also optimal for all other leaves. Thus, according to Eqn 7, the optimal divergence angle in the limiting case $B = 0°$ (cf. the discussion in the last paragraph of the previous section, and the results presented in Fig. 6a) corresponds to the solution of

$$x_{opt} \to \mathrm{Max}_x\{L_{rep}(x,0)\} = \mathrm{Max}_x\{\mathrm{Inf}_n(n \cdot |x \cdot n - [xn]|)\} \qquad (8)$$

In this form the optimization is a problem of number theory. Due to a theorem of Hurwitz and its generalizations (Prasad 1948; Cassels 1957), this has a unique solution in the interval [0,1/2] (see Appendix).

$$x_{opt} = \frac{3 - \sqrt{5}}{2}$$

that is, the golden section, that corresponds to $\alpha_{opt} = x_{opt} \cdot 360° = 137.5\ldots°$, namely the golden angle. By number theory it can be shown that the golden section has the very worst rational approximations which means it is least well approximated by rationals, i.e. truncated continued fractions (see Appendix). This ensures, according to Eqn 8, *maximal* light capture if the divergence angle equals the golden angle.

DISCUSSION

We have analysed the phyllotactic spiral under the assumption that evolutionary pressure has driven plants to optimize light capture under natural conditions which guarantees maximal photosynthetic activity, and thereby maximal carbon gain. With two quite natural and simple assumptions for plants which receive light mainly coming in parallel to the leaf stem, we can derive the 'shadow function' which represents the shadow thrown upon a lower leaf by leaves above, and thus diminishes light capture for the lower leaf. Summing over all leaves above the lowest, one obtains the total shadow function for the lowest leaf in its dependence on the divergence angle of the phyllotactic spiral. The inverse, the light capture function, measures the light capture as function of the divergence angle. Comparing this function with empirical results obtained by Pearcy & Yang (1998) from data on the Redwood understorey plant *A. bicolor* with the architecture model YPLANT (Pearcy & Yang 1996) shows an almost perfect fit of our model over the whole divergence angle range. The qualitative behaviour of our light capture model is preserved when one simplifies it according to Eqn 7. In particular, the global optimum of the simplified model lies close to the optimum obtained from numerical evaluation of the full model, corresponding to Eqn 3, and the data of Pearcy & Yang (1998). Application of number theory then shows that within our model, the golden angle is the divergence angle for maximum light capture, and that this limit will be more and more approached with decreasing leaf width and increasing total leaf number.

We stress light capture as the selective pressure in the evolution of spiral phyllotaxis optimizing Darwinian fitness, and we present a mathematical model together with analytical solutions which agree with experimental observations and an empirical model (Pearcy & Yang 1998). However, one may ask why identical rules of phyllotaxis not only apply to vegetative photosynthesizing shoots but also to reproductive shoot structures, such as flowers and cones of cycads and conifers, angiosperm flowers, capitulae (Asteraceae), etc. Is it then not a packing problem after all? One must, however, recall that reproductive structures evolved from leaves. This is still seen in extant fern allies, i.e. basic cormophyte taxa such as *Lycopodium* and *Selaginella*, where spirally arranged leaflets at the tip of the shoots bearing the sporangia in their axils mark the very early stages of flower evolution (Ehrendorfer 1998a). With respect to our theoretical finding that the golden angle increasingly perfectly optimizes light capture as leaf width decreases, it is also interesting to note that the basic taxa *Lycopodium* and *Salaginella* have rather narrow photosynthetic leaves spirally arranged on their shoots. Phylogenetically the early leaves in these groups of Pteridophyta (Lycopodiopsida) evolving primordial flowers certainly were microphylls, in contrast to the mega- or macrophylls in the other Pteridophyta, namely the ferns (Pteridopsida) in which flowers did not evolve (Ehrendorfer 1998b).

In conclusion, we can explain the observed and long-standing mystery of the golden angle in phyllotaxis with quite natural assumptions on leaf sequence and shadow casting by an appeal to the result of number theory that the 'golden mean' is characterized by the 'most irrational number'. Thus, strong evolutionary profit explains the occurrence of divergence angles close to the golden angle in nature and this aspect goes beyond the level of optimal primordial packing at the shoot apex. The fact that the mathematical result of nature's optimization coincides with that of aesthetical perception must remain intriguing.

ACKNOWLEDGMENTS

The authors are most grateful to Dr R. W. Pearcy for discussions and for communicating their original data to us. We also thank Dr K. H. Kohrs from the Studienstiftung des deutschen Volkes who facilitated this collaboration in the stimulating atmosphere of a summer university.

REFERENCES

Adler I., Barabe D. & Jean R.V. (1997) A history of the study of phyllotaxis. *Annals of Botany* **80,** 231–244.

Bonnet C. (1754) *Recherche sur l'Usage des Feuilles dans les Plantes.* E. Luzac, fils, Göttingen and Leyden.

Braun A. (1831) Vergleichende Untersuchung über die Ordnung der Schuppen an den Tannenpflanzen als Einleitung zur Untersuchung der Blattstellung überhaupt. *Nova Acta Ph Medical Academy of Cesar Leop Carolina Nat Curiosorum* **15,** 195–402.

Bravais L. & Bravais A. (1837) Essai sur la disposition des feuilles curvisériées. *Annals of Science Nat Botany Biology Vég* **7,** 42–110,193–221, 91–348; **8,** 11–42.

Cassels J.W.S. (1957) *An Introduction to Diophantine Approximation* Cambridge University Press, Cambridge, UK.

Cummings F.W. & Strickland J.C. (1998) A model of phyllotaxis. *Journal of Theoretical Biology* **192,** 531–544.

d'Ovido F. & Mosekilde E. (2000) Dynamical system approach to phyllotaxis. *Physical Review E* **61,** 354–365.

Ehrendorfer F. (1998a) Evolution und Systematik. In *Strasburger. Lehrbuch der Botanik*, 34th edn, pp. 652–654. Gustav Fischer Verlag, Stuttgart, Jena, New York.

Ehrendorfer F. (1998b) Evolution und Systematik. In *Strasburger. Lehrbuch der Botanik*, 34th edn, pp. 687–688. Gustav Fischer Verlag, Stuttgart, Jena, New York.

Fejes Tóth L. (1953) *Lagerungen in der Ebene, Auf der Kugel und Im Raum* Springer, Berlin, Germany.

Jean R.V. (1994) *Phyllotaxis – a Systematic Study of Plant Morphogenesis* Cambridge University Press, Cambridge, UK.

Kravitz S. (1967) Packing cylinders into cylindrical containers. *Mathematical Magazine* **40,** 65–71.

Meinhardt H. (1984) Models of pattern formation and their application to plant development. In *Positional Controls in Plant Development* (eds P.W. Barlow & D.J. Carr), pp. 1–32. Cambridge University Press, Cambridge, UK.

Melissen H. (1994) Densest packings of eleven congruent circles in a circle. *Geometriae Dedicata* **50,** 15–25.

Pearcy R.W. & Yang W. (1996) A three-dimensional crown architecture model for assessment of light capture and carbon gain by understory plants. *Oecologia* **86,** 1–12.

Pearcy R.W. & Yang W. (1998) The functional morphology of light capture and carbon gain in the Redwood forest understory plant *Adenocaulon bicolor* Hook. *Functional Ecology* **12,** 543–552.

Prasad A.V. (1948) Note on a theorem of Hurwitz. *Journal of London Mathematical Society, Series I* **23,** 169–171.

Schimper C.F. (1836) Geometrische Anordnung der um eine Axe periferischen Blattgebilde. *Verhandl Schweiz Naturf Ges* **21,** 113–117.

Schürmann A. (2002) On Extremal Finite Packings. *Discrete Computational Geometry* **28,** 389–403.

Sitte P. (1998) Morphologie. In *Strasburger. Lehrbuch der Botanik*, 34th edn, pp. 158–159. Gustav Fischer Verlag, Stuttgart, Jena, New York.

Received 27 August 2003; received in revised form 11 December 2003; accepted for publication 5 February 2004

APPENDIX

Number theoretical relations

The Hurwitz theorem

The Hurwitz theorem is concerned with approximations of real numbers x by fractions. The best approximating fraction with denominator n is $[x \cdot n]/n$, and we have $|x - [x \cdot n]/n| \leq 1/n$ by definition of $[x \cdot n]$. A deeper study shows that in fact $|x - [x \cdot n]/n| \leq h/n^2$ for some constant h depending on x. Equivalently, $n|x \cdot n - [x \cdot n]| \leq h$. The Hurwitz theorem tells us how close the approximation can be, since it provides estimates for $n|x \cdot n - [x \cdot n]|$.

The Hurwitz theorem is based on the representation of real numbers by continued fractions. Any positive real number x has a (possibly infinite) continued fraction expansion

$$x = a_0 + \cfrac{1}{a_1 + \cfrac{1}{a_2 + \cfrac{1}{\cdots}}} = [a_0, a_1, a_2, \ldots]$$

with an integer a_0 and natural numbers a_1, $a_2, \ldots$ A finite continued fraction is rational. The fraction $p_m/q_m = [a_0, a_1, a_2, \ldots, a_m]$ is called the m-th partial quotient of x. With these definitions we state parts of the theorem of Hurwitz and its generalizations. Details are given in (Cassels 1957).

1 For infinitely many n holds $n \cdot |x \cdot n - [x \cdot n]| < 1/\sqrt{5}$. In general, the constant $1/\sqrt{5}$ can not be replaced by any smaller constant.

2 If $n \cdot |x \cdot n - [x \cdot n]| < 1/\sqrt{5}$ then $n = q_m$ for some m. In other words, the best approximations of x are the partial quotients of x.

3 It holds $\mathrm{Inf}_n\{n \cdot |x \cdot n - [x \cdot n]|\} = 2/(3 + \sqrt{5}) \approx 0.382$ if and only if $x = [a_0, a_1, 1,1,1, \ldots]$ with $a_1 = 1$ or $a_1 = 2$. For all other numbers $\mathrm{Inf}_n\{n \cdot |x \cdot n - [x \cdot n]|\} < 6/17 \approx 0.353$.

Statement 3 implies that the unique solution of Eqn 8 in the interval [0,1/2] is $x_{\mathrm{opt}} = [0,2,1,1,1, \ldots] = (3 - \sqrt{5})/2$.

Statements 1 and 2 can be found in (Cassels 1957), and the first part of statement 3 is proved in (Prasad 1948). The proofs are based on the equation

$$q_m(xq_m - [xq_m]) = \frac{(-1)^m}{[a_{m+1}, a_{m+2}, a_{m+3}, \ldots] + [0, a_m, a_{m-1}, \ldots, a_1]}$$

which holds for any $m \geq 1$. The equation essentially means that there are good approximations of x if there are big coefficients in its continued fraction expansion. The second part of statement 3 is a straightforward application of this equation. It ensures that the ratio of the optimal light capture, obtained at the golden angle and at the next optimal angles is greater than 1.082, a result borne out also by the numerical evaluations, see Fig. 6.